EFFECT OF FLUX RATIO IN FLUX-CORED WIRE ON WIRE MELTING BEHAVIOUR AND FUME EMISSION RATE




E. Yamamoto **K. Yamazaki** **K. Suzuki** **F. Koshiishi**

ABSTRACT

In GMAW, the welding wire melts itself due to the arc discharges from the electrode. Both the Joule heating and the arc heating of the electrode contribute to the melting of the wire. In general, it is said that flux-cored wire (FCW) melts faster than solid wire as the welding current flows mainly through the sheath of the FCW. FCW structure differs from solid wire and these differences affect not only the wire melting behaviour, but also the fume emission rate (FER). However, at present, no report exists which defines these effects in detail. Therefore, it is very important to clarify the effect of these differences in wire structure on the wire melting behaviour and FER in order to understand how to reduce the latter. In this study, we found that FER increased with the flux ratio of FCW. It is assumed that these results can be attributed to the state of the stability of the flux column in the arc and the heat content of the droplets.

IIW-Thesaurus keywords: *Cored filler wire; Fume control; Heat; Metal transfer; Process parameters; Stick out.*

1 BACKGROUND AND PURPOSES

In GMAW, the wire melting rate governs the welding efficiency [1]. Because FCW has the feature of high deposition rates as well as good usability, the consumption of FCW has rapidly increased in recent years. On the other hand, developments in the FCW welding process and FCW with low fume emission have been strongly demanded [2, 3]. A lot of research into solid wire has long been conducted and it has been clarified that the molten metal transfer mode and the rate of short circuit greatly affect the fume emission phenomenon [4, 5]. Based on these findings, various new processes including the output waveform control have been achieving a drastic decrease of fume emission. By contrast, the mechanism of FCW fume emission has not yet been clarified. This is because the structure of FCW is not as simple as that of solid wire, as it is composed of a metal sheath and a flux that consists of various materials. Hence, in order to find a principal guide to clarify the fume emission mechanism, the authors have studied the effect of the droplet heat content on the fume emission rate of some FCW testing wires of different flux ratios.

Ms. Eri YAMAMOTO (yamamoto.eri@kobelco.com), Research Engineer, Mr. Kei YAMAZAKI (yamazaki.kei@kobelco.com), Research Engineer, Mr. Keiichi SUZUKI (suzuki.keiichi@kobelco.com), Senior Researcher Engineer and Mr. Fusaki KOSHIISHI (koshiishi.fusaki@kobelco.com), General Manager, are all with Kobe Steel Ltd, Welding Business, in the Technical Development Dept., Kanagawa (Japan).

Doc. IIW-1955-08 (ex-doc. XII-1936r1-08), recommended for publication by Commission XII “Arc Welding Processes and Production Systems.”

2 MEASURING METHOD FOR FUME EMISSION RATE

The fume emission rate was measured with the suction method, using the air sampler according to ISO 15011-1 [6]. Figure 1 shows a schematic diagram of the fume collecting system used for this experiment. Bead-on-plate welding was carried out in the fume collecting box for 30 s, then the fumes generated were

sucked in by the air sampler for 3 min and 30 s. To filter the fumes, a filter (made by Pall Company) was used during the suction. The fume emission rate per unit time *Ft* (mg/min.) was determined by the difference in the mass of the filter measured before and after welding. The fume emission rate was measured 3-5 times for each testing wire. The testing wires were welded on the base metal of SM490, using a welding speed of 30 cm/min, a tip-to-base metal distance of 25 mm and a shielding gas of 100 %CO_2 at 25 l/min.

3 EFFECT OF FCW FLUX RATIO ON FUME EMISSION RATE

3.1 Testing wires

Table 1 shows the specifications of the testing wires which were made of steel strip, with the same size and chemical composition, and of cored flux with the same composition.

Table 2 shows the cross-sections of the testing wires. As shown in the table, the ratio of sheath area R_h (%) to the entire cross-section of the wire decreases with the increase in the flux ratio. The R_h values shown in the table were computed by an image-analyzing software. For each wire, six samples were photographed to measure the R_h values and the average values are shown in the table.

3.2 Fume emission rate per unit time

The effect of welding current on the fume emission rate per unit time for each testing wire is shown in Figure 2. For this test, the FER from the weld pool is not taken into account because the surface temperature of weld metal in CO_2 arc welding was measured at around 1 800 K which is less than the boiling point of the mild steel though the temperature of the droplet surface ranges from 2 000 K to 3 000 K [7]. Therefore, the fume generation from the droplet is dominant compared to the one from the weld pool. The fume emission rates were measured with the appropriate voltage for each welding current. The appropriate arc voltage was set at minimum spatter and fume generation rate by visual observation. The arc voltage, wire feed rate and droplet transfer mode are shown in Table 3. As shown in Figure 2, the FER rate increases as the flux ratio increases. Also, the weight of consumed wire per unit time was measured at the same wire feed speed for each welding condition as when the FER was measured.

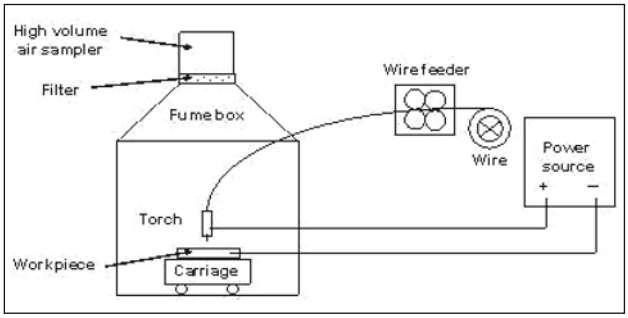

Figure 1 – Schematic diagram of fume collecting system

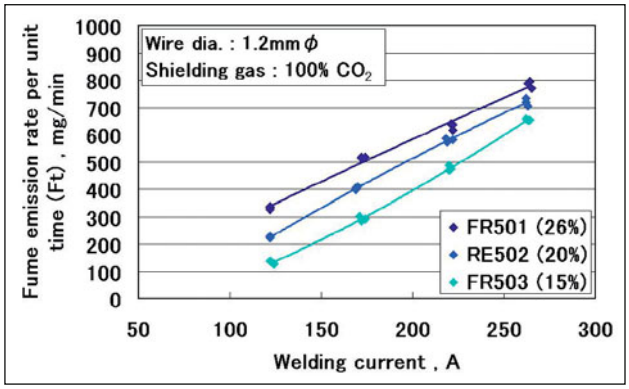

Figure 2 – Effect of welding current on fume emission rate per unit time

Table 1 – Specifications of testing wires

Wire	Diameter of wire	Flux	Flux ratio
FR501	1.2 mm	Rutile-base	26 %
FR502			20 %
FR503			15 %

Table 2 – Cross-sectional views of the testing wires and the ratio of sheath cross-section to the entire cross-section of wire

Wire	FR501	FR502	FR503
Wire cross-section	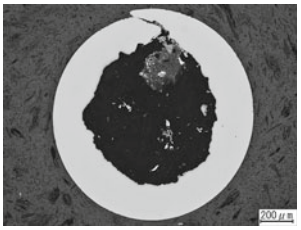	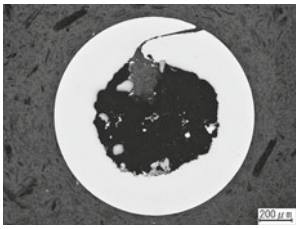	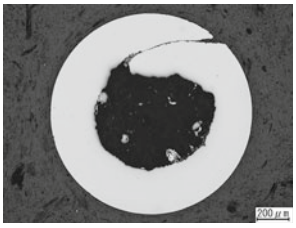
Rh [%]	58.6	63.0	70.1

Table 3 – Welding condition and droplet transfer

Welding current [A]	Wire	Arc voltage [V]	Wire feed rate [m/min]	Droplet transfer
120	FR501	23.8	5.4	S
	FR502	21.4	4.8	S
	FR503	19.5	4.4	S
170	FR501	25.7	9.0	S-D
	FR502	24.6	7.4	S-D
	FR503	23.5	6.9	S-D
220	FR501	28.5	13.2	D
	FR502	26.8	11.0	D
	FR503	26.4	9.6	D
260	FR501	32.3	18.0	D
	FR502	30.0	14.5	D
	FR503	28.5	12.7	D

Note **S**: Short-circuiting transfer, **D**: Drop transfer.

This can be seen in Figure 3. All measurements of wire melting rate against welding current were carried out manually without arc discharge. As shown in Figure 3, the wire melting rate increases with the increases in flux ratio. This is because, as shown in Table 2, the R_h value decreases as the flux ratio increases and therefore the Joule heat increases.

4 HEAT CONTENT IN FCW MOLTEN METAL DROPLET

The factors that affect the fume emission rate include the heat content of the molten metal droplet H_0 (J/mm^3) and the molten metal transfer mode. The heat content of the molten metal droplet with the testing wires of various flux ratios was computed using the Halmoy method [8]. Also, the molten metal transfer phenomenon was observed.

4.1 Computation method for heat content (H_0) in molten metal droplet.

In order to simplify the computation of the heat content of the molten metal droplet, the following assumption was made. For the Joule heat generated in the wire extension portion,

(1) the welding current flows only in the sheath but not in the cored flux, and

(2) the R_h shown in Table 2 was used for computing the current density.

Because the heat content (H_0) of the molten metal droplet is the summation of the heat content per unit volume of droplet received in stick-out (Joule heat) H_L and the heat content per unit volume of droplet received at anode tip H_A, it can be expressed by the following equation.

$$H_0 = H_L + H_A \quad (1)$$

Considering the calculation system shown in Figure 4, the rate of heat change H per unit time can generally be shown by the following equation.

$$\frac{dH}{dt} = V\frac{dH}{dx} = \rho(H)j^2 \quad (2)$$

Using Equation (2), the integration of a nominal wire length of *dx,* from the tip of the contact tube to the wire tip can be given by the following equation.

$$\int_0^L dx = \frac{V}{j^2}\int_0^{H_L}\frac{dH}{\rho(H)} \quad (3)$$

And the following equation can be obtained.

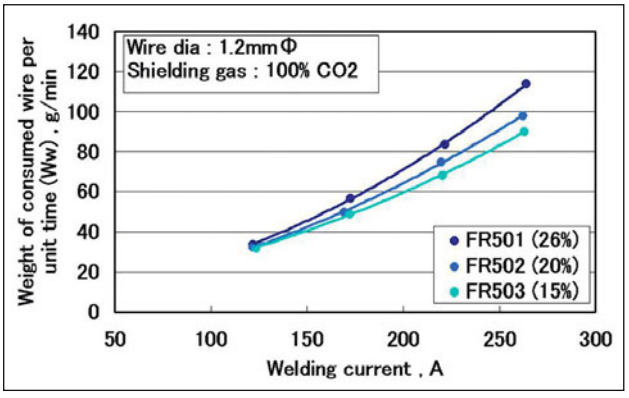

Figure 3 – Effect of welding current on wire melting rate

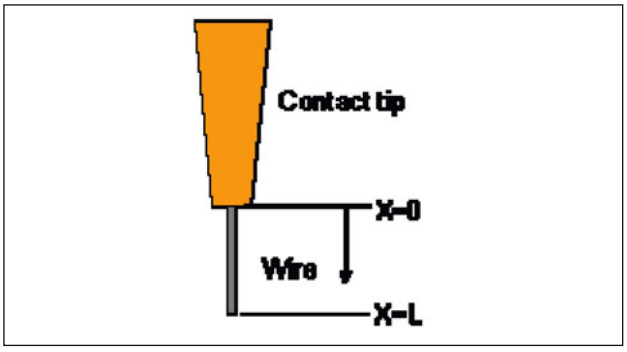

Figure 4 – Wire extension portion

$$\frac{Lj^2}{V} = V\int_0^{H_L}\frac{dH}{\rho(H)} = f(H_L) \tag{4}$$

The voltage V_L of the wire extension portion is given by Equation (5) and so Equation (6) can be obtained.

$$V_L = j\int_0^L \rho dX = \frac{V}{j}\int_0^{H_L} dH = \frac{V}{j}H_L \tag{5}$$

$$H_L = \frac{jV_L}{V} \tag{6}$$

When electric current flows in a wire of length L with a constant-current power source, the $f(H_L)$ at t_1 (seconds) after starting the current flow can be obtained by Equation (7), taking into account the time response of the voltage between the ends of the wire. This allows Equation (6) to be expressed by Equation (8). In this experiment, the time response of the voltage was measured by a high-speed waveform recorder. A typical measurement of actual voltage of $V_L(t)$ is shown in Figure 5. In this case, welding currents of 200-300 A were supplied to the wire and the time integration of the voltage data was conducted for each current.

$$f(H_L) = t_1 j^2 \tag{7}$$

$$H_L = \frac{j}{L}\int_0^{t_1} V_L dt \tag{8}$$

Because Halmoy reported that $f(H_L)$ and H_L had a proportional relationship, they can be expressed by Equation (9) using constants a and b.

$$H_L = af(H_L) + b = a\left(\frac{j^2L}{V}\right) + b \tag{9}$$

The values j, L, and t_1 obtained in the experiment and the time integration value of voltage were substituted in Equations (7) and (8), respectively, and then the constants a and b were obtained from Equation (9), which are shown in Table 4. The heat content per unit volume of droplet received at anode tip H_A can be expressed by the following equation.

$$H_A = \frac{\phi j}{V} \tag{10}$$

Substitution of Equations (9) and (10) in Equation (1) results in Equation (12), which provides the relation between V, L and j.

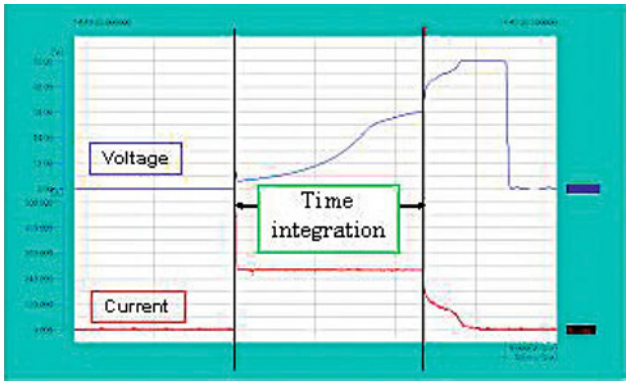

Figure 5 – Actual current and voltage in wire

Table 4 – Computation results of constants *a* and *b*

Wire	*a*	*b*
FR501	0.75×10^{-3}	1.2875
FR502	0.61×10^{-3}	0.1948
FR503	0.26×10^{-3}	5.5832

$$H_0 = H_L + H_A = a\left(\frac{j^2L}{V}\right) + b + \frac{\phi j}{V} \tag{11}$$

$$\therefore V = \frac{a}{H_0 - b}j^2L + \frac{\phi}{H_0 - b}j \tag{12}$$

In addition, the welding current was varied in the range of 140-240 A and the relationship between the wire melting rate (wire feed rate) V and the wire extension L was obtained, with the images taken by a high-speed video camera. The results are shown in Figure 6. The heat content H_0 was computed using Equation (12) and the relation between V and L obtained in Figure 6.

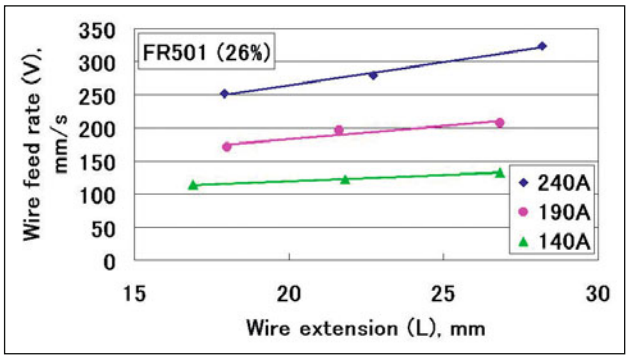

a) FR501 (26%)

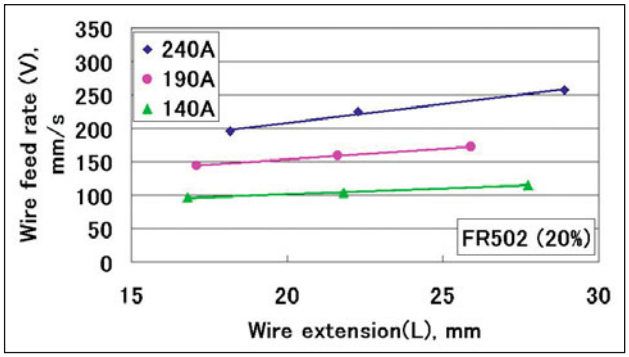

b) FR502 (20%)

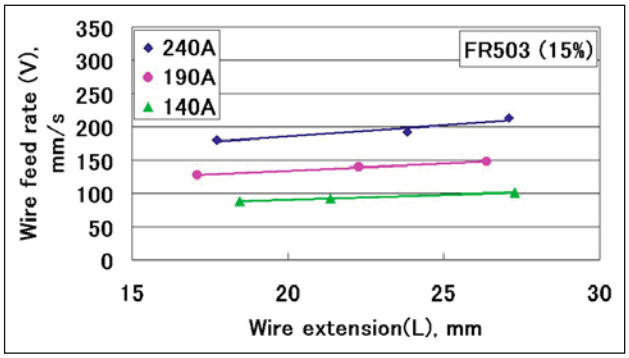

c) FR503 (15%)

Figure 6 – Relation between wire feed rate, wire extension and current

4.2 Results of heat content computation

The effect of welding current on the heat content of the molten metal droplet, computed using the process described in Section 4.1, is shown in Figure 7. At high currents, the effect of the flux ratio on the heat content is almost negligible; at low currents, the heat content increases as the flux ratio increases.

4.3 Relation between heat content, fume emission rate and molten metal transfer mode

The effect of a welding current on the fume emission rate per unit weight of consumed wire F_W is shown in Figure 8. As shown in Figures 7 and 8, both the heat content and actual fume emission rate per unit weight of consumed wire have a similar tendency in relation to the welding current; that is, the fume emission rate per unit weight of consumed wire increases with the increase in heat content. Not only the droplet heat content but the stability of the droplet transfer and the welding condition effect on FER and, in addition that, those factors which effect on FER are complexly intertwined each others. The effects of flux ratio on the heat content and FER differed at the low current and the high current. To research this phenomenon, the droplet transfer modes at welding currents of 260 and 120 A were observed using a high-speed video camera. At a high current of 260 A, both the wire melting rate and the flux melting rate were relatively large and the flux protrusion was kept stable. Therefore, the molten metal transfer mode was kept constant at all flux ratios. By contrast, at a low current of 120 A, as shown in Figure 9, the flux protrusion became thicker and longer with the increase in flux ratio, the flux stick-out was exposed to the high temperature arc and thus gas explosions were observed in the arc atmosphere. FCW includes various kinds of metal and compounds the boiling points of which are relatively low. Gasification of those materials overheated in the arc prevents the smooth droplet detachment from the wire, as well as the stable droplet transfer. As a result, the molten metal transfer became unstable and the molten metal droplet stayed on the wire tip for a longer time. In this case, it can be considered that the molten metal droplet received a larger amount of arc heat, thereby causing larger heat content, with an increase in the fume emission rate.

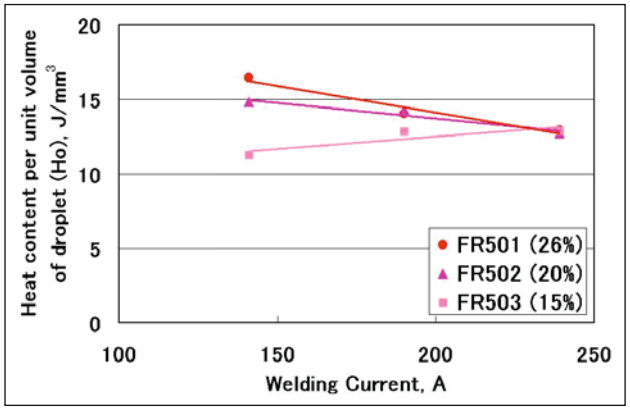

Figure 7 – Effect of welding current on heat content

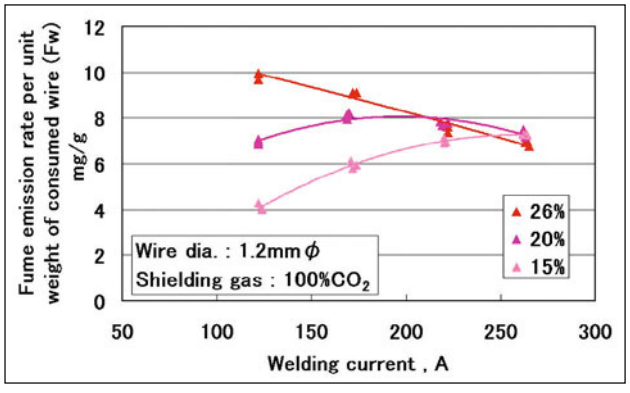

Figure 8 – Fume emission rate per unit weight of consumed wire

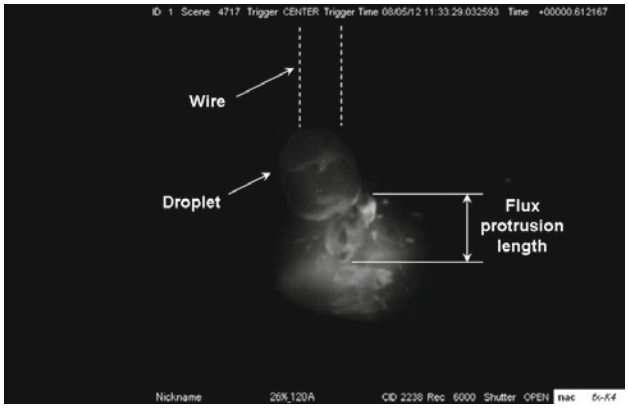

a) FR501 (26 %)

b) FR502 (20 %)

c) FR503 (15 %)

Figure 9 – Photographs of droplet in the arc (120A)

5 CONCLUSIONS

The effects of the flux ratio of FCW on the fume emission rate and the heat content of a molten metal droplet have been investigated. Consequently, it has been clarified that the fume emission rate and the heat content exhibit a similar tendency in relation to the welding current; that is, the fume emission rate increases as the heat content increases. From these results, it can be said that the heat content should be reduced to decrease the fume emission rate.

6 PARAMETERS

a, b	constants
H	heat content per unit volume [J/mm^3]
H_A	heat content per unit volume of droplet received at anode tip [J/mm^3]
H_L	heat content per unit volume of droplet received in stick-out [J/mm^3]
H_0	heat content per unit volume of droplet received at detachment [J/mm^3]
I	current [A]
j	current density [A/mm^2]
L	length or stick-out [mm] time [s]
V	wire feed rate [mm/s]
X	coordinate along stick-out [mm]
Φ	effective melting potential at anode [V]

REFERENCES

[1] Hirata Y.: Physics of Welding [III] – Melting rate and temperature distribution of electrode wire, Journal of the Japan Welding Society, 1994, vol. 63, no. 7, pp. 484-488 (in Japanese).

[2] Morimoto T.: Developments in flux-cored wire for gas shielded arc welding, Kobe Steel Engineering Reports, Sept. 2005, vol. 55, no. 2, pp. 61-65.

[3] Kurokawa T.: Past and present developments in flux-cored wire for MAG welding, Kobe Steel Engineering Reports, Dec. 2000, vol. 50, no. 3, pp. 24-77.

[4] Suga T., Kobayashi M.: Fume generation in CO_2 arc welding by solid wire, Quarterly Journal of the Japan Welding Society, 1984, vol. 2, no. 2, pp. 220-228 (in Japanese).

[5] Yamazaki K., Yamamoto E., Suzuki K., Koshiishi F., Ono K., Tashiro S., Tanaka M., Nakata K: Effects of welding process parameters on fume emission in GMAW: IIW Doc. XII-1922-07, 2007.

[6] ISO 15011-1:2009: Health and safety in welding and allied processes –Laboratory method for sampling fume and gases – Part 1: Determination of fume emission rate during arc welding and collection of fume for analysis.

[7] Halmoy E.: Wire melting rate, droplet temperature, and effective anode melting potential, Proceedings of the International Conference on Arc Physics and weld Pool Behavior, 1980, pp. 49-57.

[8] Tanaka M., Waki K., Tashiro S., Nakata K., Yamamoto E., Yamazaki K., Suzuki K.: Visualizations of 2D temperature field of molten metal in arc welding process, IIW Doc. SG-212-1122-08, 2008.